Nuclear Instruments and Methods in Physics Research A 768 (2014) 55–61

Contents lists available at ScienceDirect

Nuclear Instruments and Methods in Physics Research A

journal homepage: www.elsevier.com/locate/nima

Pulse pile-up and dead time corrections for digitized signals from a BaF_2 calorimeter

E. Mendoza [a,*], D. Cano-Ott [a], C. Guerrero [b,a], E. Berthoumieux [c,b]

[a] CIEMAT, Avda. Complutense 40, 28040 Madrid, Spain
[b] CERN, Physics Department, Geneva, Switzerland
[c] CEA/Saclay - IRFU, Gif-sur-Yvette, France

The n_TOF Collaboration[1]

ARTICLE INFO

Article history:
Received 17 March 2014
Received in revised form
22 August 2014
Accepted 5 September 2014
Available online 16 September 2014

Keywords:
Pulse pile-up
Dead time
Digitizers
Flash ADC
BaF_2 calorimeter
N_TOF

ABSTRACT

The pulse pile-up and associated dead time effects in an ^{243}Am(n,γ) cross section measurement with a BaF_2 Total Absorption Calorimeter at the CERN n_TOF facility have been characterized. In this case, reliable corrections of these effects are crucial because of the complex detector configuration and of the high count rate induced by the sample activity of 50 MBq. The techniques, which have been developed for offline processing of the present data, may be of general interest for the analysis of other experiments using digital acquisition systems.

1. Introduction

The neutron time-of-flight n_TOF facility at CERN has been built for the measurement of neutron cross sections of relevance for nuclear technologies and nuclear astrophysics. A full description of the facility can be found in [1]. One of the detectors used at n_TOF is the Total Absorption Calorimeter [2]. The TAC, shown in Fig. 1, is a segmented array composed of 40 BaF_2 crystals 15 cm in length, which covers 95% of the solid angle around the sample in the centre. This detector is used to measure neutron capture cross sections by the coincident detection of the prompt capture γ-ray cascade. Each BaF_2 crystal is coupled to a 5″ photomultiplier. The anode signals of each module are recorded by high-performance digitizers (Acqiris-DC 270) with 8 bit resolution and 8 MB memory, which were operated at 250 and 500 MSamples/s [3]. In this way, the entire digitized response of the TAC to each neutron pulse could be stored for 32 or 16 ms, respectively.

The BaF_2 signals in the digitized data buffers were identified with a special pulse shape analysis routine, returning for each signal the time-of-flight, the area corresponding to the deposited energy, and additional parameters for particle identification, i.e. to distinguish γ-rays from the intrinsic α background due to the decay of radium impurities in the crystals. This routine is described in detail in [4], and a more accessible reference of a similar routine can be found in [5]; while it's application to the BaF_2 detectors in the TAC is discussed in [2]. An example of the performance of the routine is shown in Fig. 2. After the energy calibration of all the detectors, by means of standard calibration sources, the individual signals are grouped into TAC events, using a time coincidence window of 20 ns. Each TAC event is characterized by its time-of-flight, total deposited energy (E_{sum}) and crystal multiplicity (m_{cr}), which is the number of detector modules contributing to the event above a given threshold. Conditions are applied to the detected events in E_{sum} and m_{cr} in order to improve the capture to background ratio. In the following, the term *event* is used for the coincident information characterized by E_{sum} and m_{cr}, which is composed by individual *signals*.

The analysis of the experimental data (i.e. TAC event rate as a function of the time-of-flight) leads to the experimental capture yield, defined as the fraction of incident neutrons undergoing a capture reaction in the sample, as a function of the neutron

* Corresponding author. Tel.: +34 913466614; fax: +34 913466576.
E-mail addresses: emilio.mendoza@ciemat.es (E. Mendoza), daniel.cano@ciemat.es (D. Cano-Ott), carlos.guerrero@cern.ch (C. Guerrero), Eric.Berthoumieux@cea.fr (E. Berthoumieux).
[1] http://cern.ch/nTOF

http://dx.doi.org/10.1016/j.nima.2014.09.010
0168-9002/

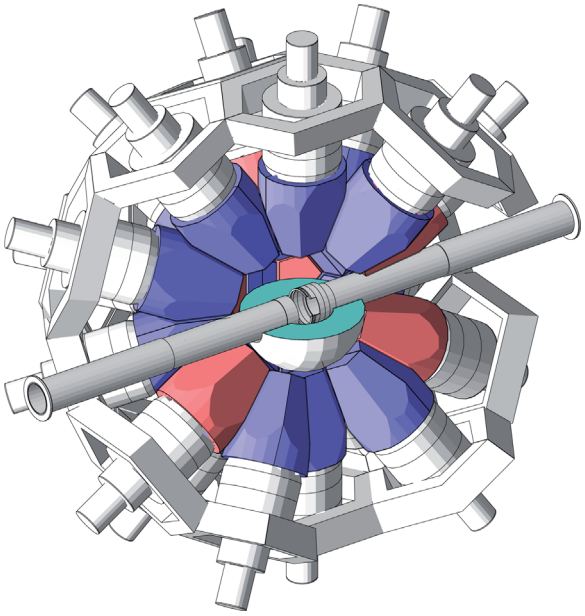

Fig. 1. Schematic view of the n_TOF Total Absorption Calorimeter.

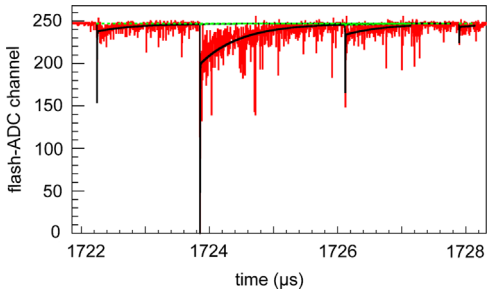

Fig. 2. Pulse shape analysis of a BaF_2 signal in the buffered digitized data.

energy, E_n. This procedure requires the determination of the experimental background and of the detection efficiency, which are obtained from dedicated measurements and from Monte Carlo calculations, respectively. These Monte Carlo calculations are described in [6], and a detailed description of an analysis performed with the n_TOF TAC can be found in [7].

One of the corrections, which have to be applied to the measured data, concerns the dead time in the detection system. This correction becomes non-negligible for counting rates higher than ~ 0.1 events/μs.[2] Because the response of each BaF_2 module is digitized every 2 or 4 ns, the detection system does not have a dead time as it is usually defined. However, if two signals are close enough, the pulse shape analysis routine can have difficulties in resolving the pulse pile-up, either in separating the two signals or in reconstructing their areas (energies) correctly. Accordingly, in this paper *dead time* is considered as the (variable) time period, within which two subsequent signals are not properly reconstructed by the pulse shape analysis routine.

During the ^{243}Am capture cross section measurement [8,9] the high activity of the sample induced a background of 5.4 events/μs in the TAC. Thus, the average time distance between two consecutive signals in one crystal is around 7.4 μs,[3] which is only 12 times the 620 ns time constant of the slow component in the scintillation light of BaF_2.

For experiments with such high event rates, new techniques have been developed to characterize and correct for the pulse pile-up and associated dead time effects. In particular, three situations are difficult to handle:

1. Effect of the sample activity on other background components. The background in the TAC measurements, $C_{bkg}(E_n)$, is obtained from dedicated measurements. However, during the ^{243}Am sample measurement the detection of the background events is distorted by the dead time induced by ^{243}Am sample activity, whereas in the background measurement (in absence of the sample) they are not. Therefore, the background from the dedicated measurements can not be subtracted directly from the capture data. In other words, if the different sources of background are measured separately ($C_{bkg,1}(E_n)$, $C_{bkg,2}(E_n)$, …) and the counting rates are low, then the total background (all the sources measured together) can be calculated as $C_{bkg}(E_n) = C_{bkg,1}(E_n)+C_{bkg,2}(E_n)+\ldots$. If the counting rates of any of the background sources is high, as in case of a highly radioactive sample, then it will affect the detection of the other background sources, and the overall background is no longer the same as the sum of the different components.
2. Effect of the sample activity on the detection of capture cascades. The efficiency is obtained from Monte Carlo simulations including the generation of the capture cascades, the transport of the γ-rays in the TAC geometry, and the reconstruction of the detected events. The high background rates affect the detection of the capture events in the real experiment, since the probabilities of random summing or pulse pile-up are sizable and need to be considered in the simulation.
3. Effect of overlapping capture cascades. If the capture rates are high, e.g. in case of strong resonances, the possible overlap of capture cascades must be corrected in the calculation of the capture yield.

The techniques, which have been developed for the three cases, are presented in the following sections.

2. Effect of the sample activity on other background components

The background of the ^{243}Am(n,γ) cross section measurement is determined by two main components:

1. The ambient background and the background due to the sample activity are constant in time, independent of the neutron beam, and can be measured in separate beam-off runs, with and without the ^{243}Am sample.
2. The beam-related background can be divided in (i) the interaction of the neutrons with the ^{243}Am sample (the scattered neutrons can be captured in the TAC); (ii) the interaction of the neutrons with the Ti canning of the ^{243}Am sample;[4] and (iii) the rest of the contributions. Contribution (i) is determined by replacing the ^{243}Am sample by a graphite sample to simulate the effect of scattered neutrons [7], while (ii) and (iii) are deduced from dedicated measurements without the ^{243}Am sample and with and without a Ti can. The background runs for measuring (ii) and (iii) are labeled further on as “Ti canning” and “empty frame”, respectively.

[2] Note that an *event* is a coincidence performed with individual *signals*.

[3] Because most events due to the sample activity have $m_{cr} = 1$, the count rate in the individual modules is around $5.4/40 = 0.14$ signals/μs on average.

[4] The sample consisted of an AmO_2 pellet highly enriched in ^{243}Am, deposited in an Al layer and encapsulated in a welded Ti can.

Pile-up of γ-rays from the decay of ^{243}Am is distorting the energy distribution and the number of detected background counts during the capture measurement. However, the dedicated background measurements without ^{243}Am are not distorted by the sample activity, thus preventing an accurate background subtraction. Therefore, the effect of the sample has been simulated by creating artificial data by mixing the digitized signals from the background measurements with signals from the ^{243}Am activity measurement (^{243}Am sample in place, but without neutron beam). These simulated background data were then analyzed in the same way as the real data taken with the ^{243}Am sample.

The two data sets were combined, first by calculating the baseline values b_1, b_2. Then, the signal amplitudes at each point i in the new data buffer were calculated with 8 bit resolution according to $a_{Sum,i}=a_{1,i}+a_{2,i}-(b_1+b_2)/2$, where $a_{1,i}$ and $a_{2,i}$ are the amplitude signals in the first and second data buffers. If the resulting value was negative or greater than 255 it was set to 0 or 255, respectively.

The artificial data buffers created with this procedure correspond to a background measurement performed together with the detection of the sample activity, except that the ambient background (measured without sample and without neutron beam) has been counted twice.

The procedure has been validated by comparing the resulting deposited energy spectra in the TAC (E_{sum}) measured with the sample (^{243}Am), with the Ti canning only (TiCan), and the artificial spectrum combining the Ti background and the sample activity (Rad_TiCan). In all spectra shown in Fig. 3, events from neutron interactions in other elements than the sample or the Ti canning have been subtracted. It should be noticed that all the events above $E_{sum}=6$ MeV correspond to the interaction (elastic scattering or capture) of neutrons in the Ti canning, because the total capture-cascade energies from ^{243}Am are limited by the neutron separation energy of $S_n=5.36$ MeV in ^{244}Am, and because background events without beam have even lower energies.

As shown in Fig. 3, there is a sizeable difference between the deposited energy spectrum corresponding to the Ti canning in the ^{243}Am measurement (^{243}Am) with the one obtained in the background measurement (TiCan). When the corrections described in this section are applied (Rad_TiCan), the difference disappears. Note that the discrepancies below 6 MeV are due to capture events in ^{243}Am and, therefore, not relevant in the background discussion. The spectra shown in Fig. 3 correspond to incident neutron energies between 10 and 100 eV, and events for all the detected multiplicities have been considered ($m_{cr}>0$). However, similar results are obtained at other neutron energies and considering different conditions in the crystal multiplicity.

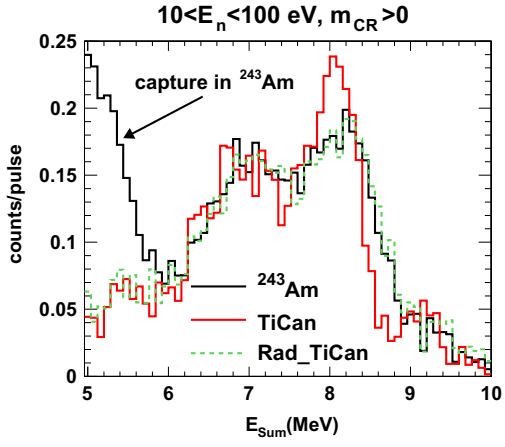

Fig. 3. Deposited energy spectra in the neutron energy range from 10 to 100 eV and all multiplicities. The effect of the Ti canning in the measurement with sample (^{243}Am) has been successfully determined with the corrections described in this section (Rad_TiCan), whereas significant differences are found in a background run with the Ti canning alone (TiCan).

3. Effect of the sample activity on the detection of capture cascades

The dead time induced by the sample activity affects the detection of capture cascades and is thus important with respect to the overall TAC efficiency. The efficiency is obtained by Monte Carlo simulations, including a realistic event generator for the electromagnetic de-excitation of the compound nucleus [10], the transportation of the generated cascades in the TAC geometry with a code based in the GEANT4 package [11], and the reconstruction of the detected events, which is performed in the same way as it is done for the real experimental data. A detailed description of the methodology and its validation is given in [6].

The detection of a capture event can be affected by another event if both are close in time. Such an event can be (i) a different capture event or (ii) a background event. The first case may be important in the vicinity of a strong resonance, where the counting rate can increase significantly, and it will be treated in Section 4. The second case is usually negligible, except when the sample activity is high enough to affect the detection of the capture cascades. The dead time associated to other sources of background with lower counting rates has been neglected.

There are two situations where capture events are affected by the high sample activity:

1. Signals from the sample activity are detected in one or more BaF_2 crystals in coincidence with a capture event. In this case, although the detection of the individual capture signals is not affected, the total energy of the capture event and its multiplicity are increased, thus modifying the TAC detection efficiency, which depends on the E_{sum} and m_{cr} conditions considered.
2. The detection of an individual capture γ-ray is affected by a background signal, if both γ-rays hit the same BaF_2 close in time. In this case, it is possible to miss or detect a capture γ-ray with the wrong energy, thus distorting the entire event.

The first effect has been taken into account in the reconstruction of the Monte Carlo results by adding experimental data from the ^{243}Am activity measurement to the simulated data in a random way by taking the experimental count rate (5.4 events/μs), as well as the distributions of the total deposited energy and of the event multiplicitiy into account.

The second effect was considered by combining capture data taken with the ^{197}Au sample (used for normalization) with the background data from the activity of the ^{243}Am sample. The raw data buffers of both measurements were mixed in the same way as described in Section 2. Then, the resulting artificial data buffers were analyzed with the pulse shape analysis routine, and compared with the analysis of the real ^{197}Au measurement. This procedure allows one to study the differences in the signals with and without the effect of the sample activity in the entire γ-ray energy range of interest and for all the BaF_2 detectors.

For each signal detected by the analysis routine in the ^{197}Au buffer, it was verified if a signal was detected in the new buffer at the same time or if it was masked by a background signal from the ^{243}Am activity. If detected, the difference between the reconstructed energies of the original and the distorted signals was computed.

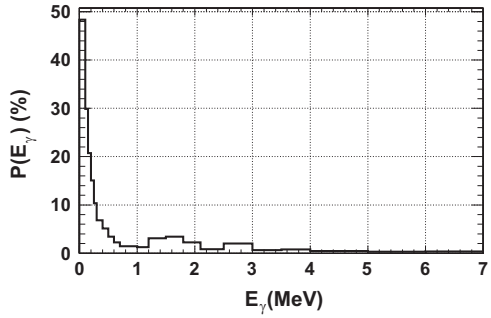

Fig. 4. Probability of not detecting a γ-ray due to the dead time effects induced by the sample activity as a function of E_γ , averaged over all BaF2 crystals.

In this way, the effect of the background due to the sample activity was characterized by

1. a function $P_{cr}(E_\gamma)$, which provides the probability that the analysis routine does not detect a γ-ray signal in a given BaF_2 crystal *cr* due to the background induced by the ^{243}Am activity, as a function of the detected energy of the signal, E_γ. This function, averaged over all the BaF_2 crystals, is presented in Fig. 4. As expected, as higher is the energy of the γ-ray, lower is the probability of not detecting it due to the sample activity;
2. a distribution $P_{E_\gamma}(\Delta E_\gamma)$, which provides the probability for $\Delta E_\gamma = E_{\gamma,rad} - E_\gamma$, where E_γ is the detected energy of the signal without ^{243}Am activity and $E_{\gamma,rad}$ the detected energy of the signal when it is distorted by a signal due to the activity of the ^{243}Am sample. In this case, the result has been averaged over all the crystals. The parametrization of the distribution in terms of E_γ was performed by dividing the energy range of interest in 27 intervals[5] and calculating a $P_{E_\gamma}(\Delta E_\gamma)$ distribution for each of these intervals. Some examples of these distribution functions can be found in Fig. 5. As it can be observed, the γ-rays are usually (but not always) detected with higher energies when they are under the effects of the ^{243}Am sample activity. As higher are the energies of the γ-rays, higher are the shifts of the detected energies (in absolute value).

These functions, $P_{cr}(E_\gamma)$ and $P_{E_\gamma}(\Delta E_\gamma)$, are used in the reconstruction of the Monte Carlo data: $P_{cr}(E_\gamma)$ is used to determine, for every signal, if the simulated signal is detected or not; and the $P_{E_\gamma}(\Delta E_\gamma)$ is applied to each detected signal, to randomize the detected energy.

This procedure has been validated with the Ti canning measurement. Between 1 and 10 eV, 95% of the neutron captures in the Ti capsule are produced in ^{48}Ti. In this isotope the levels and branching ratios of the compound nucleus ^{49}Ti are well known below the neutron separation energy, so an experimental de-excitation pattern can be used.[6] In the left panel of Fig. 6 the contribution of the Ti canning to the deposited energy spectra (TiCan) is presented together with the results of the Monte Carlo simulations (dotted lines) for different multiplicities. The experimental spectra, which have been obtained from the dedicated Ti canning measurement, after subtracting properly the rest of the background contributions, are well reproduced by the simulation, except at energies below 1.5 MeV, due to the subtraction of the background. In the right panel, the same deposited energy spectra are presented, but with the treatment presented in Section 2 (Rad_TiCan), i.e., the experimental data buffers have been mixed with signals due to the ^{243}Am activity before final analysis. This mixing was applied to the Ti canning measurement and also to the other background contributions. Again, the measured spectra are well reproduced by the corresponding Monte Carlo simulations, which are similar to the ones which appear in the left panel, but with the corrections described in this section.

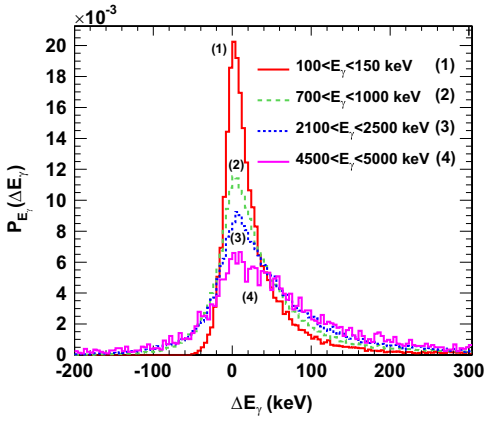

Fig. 5. Shift of the detected energy of an individual γ-ray signal due to the sample activity.

As demonstrated by the two cases in Fig. 6, the spectra of the Ti capture cascades are significantly affected by the background due to the ^{243}Am activity. In fact, 7%, 5%, 1.7%, and 1.4% of the capture cascades are missed for multiplicities greater than 0, 1, 2, and 3, respectively. (These results refer to the range of total deposited energies E_{sum} between 2.5 and 6 MeV as used in the analysis of the ^{243}Am(n,γ) measurement). It is important to note that in both cases the experimental results are well reproduced by the simulations, thus validating the procedure presented in this section. A similar comparison has been performed with the ^{197}Au measurement, finding also a satisfactory agreement between the simulations and the experimental results.

4. Effect of overlapping capture cascades

The effect of overlapping capture signals becomes important in or near strong resonances, when capture rates exceed $\sim$0.1 events/μs. The capability of the pulse shape analysis routine to identify consecutive signals has been tested with respect to the signal energies and time differences. The method is using a certain number of isolated γ-ray signals free of any pile-up distortion by other γ-rays or α-particles. The signals have been taken for all BaF_2 modules and are covering the entire energy range of interest, i.e. from 100 keV to 10 MeV. Pairs of these signals with well-defined amplitudes and time differences were added into new artificial buffers. The analyses of the artificial buffers and of the isolated signals could then be compared to characterize the dead dime effects from overlapping cascades.

As an example, the pulse shape analysis of two signals separated by different time distances are presented in Fig. 7. While the top left panel represents the case of isolated signals, the first signal in the top right panel affects the shape of the second one in such a way that the pulse shape analysis routine is not capable of detecting it as an individual γ-ray signal. In the bottom left panel, both signals are detected, but their energies have been changed significantly. Finally, in the bottom right panel, the second signal is not detected and the reconstructed energy value of the first signal is close to the energy sum of the isolated signals.

For the analysis of the ^{243}Am(n,γ) measurement 50 isolated signals were stored from each BaF_2 detector in the 27 energy

[5] The boundaries of these intervals were: 50, 100, 200, 300, 400, 500, 600, 700, 800, 900, 1000, 1200, 1400, 1600, 1800, 2000, 2300, 2600, 3000, 3400, 3800, 4200, 4600, 5000, 5500, 6000, 6500, 7000 keV.

[6] For most of the nuclei (^{198}Au and ^{244}Am, for example) the levels and branching ratios are not well known above a certain excitation energy and statistical models are used to simulate the de-excitation above this energy. These models depend on parameters, which are adjusted until the experimental results are reproduced.

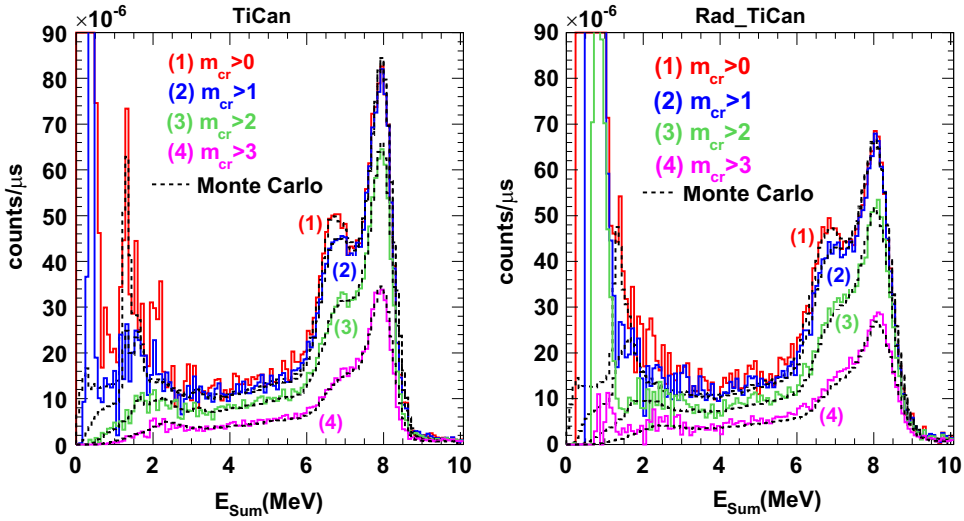

Fig. 6. Contribution of the Ti canning to the deposited energy spectra without (left) and with (right) the effects of the ^{243}Am sample activity, in the neutron energy range between 1 and 10 eV and for different multiplicities. For both cases, the simulated results are indicated by dotted lines. Note that the detection efficiency decreases with increasing multiplicity. The uncertainties in the experimental data (histograms with 60 keV/bin) are, on average, 13% ($m_{cr}>0$) and 11% ($m_{cr}>3$) in the 3–6 MeV energy range, and 4% ($m_{cr}>0$) and 6% ($m_{cr}>3$) in the 6-8.5 MeV energy range.

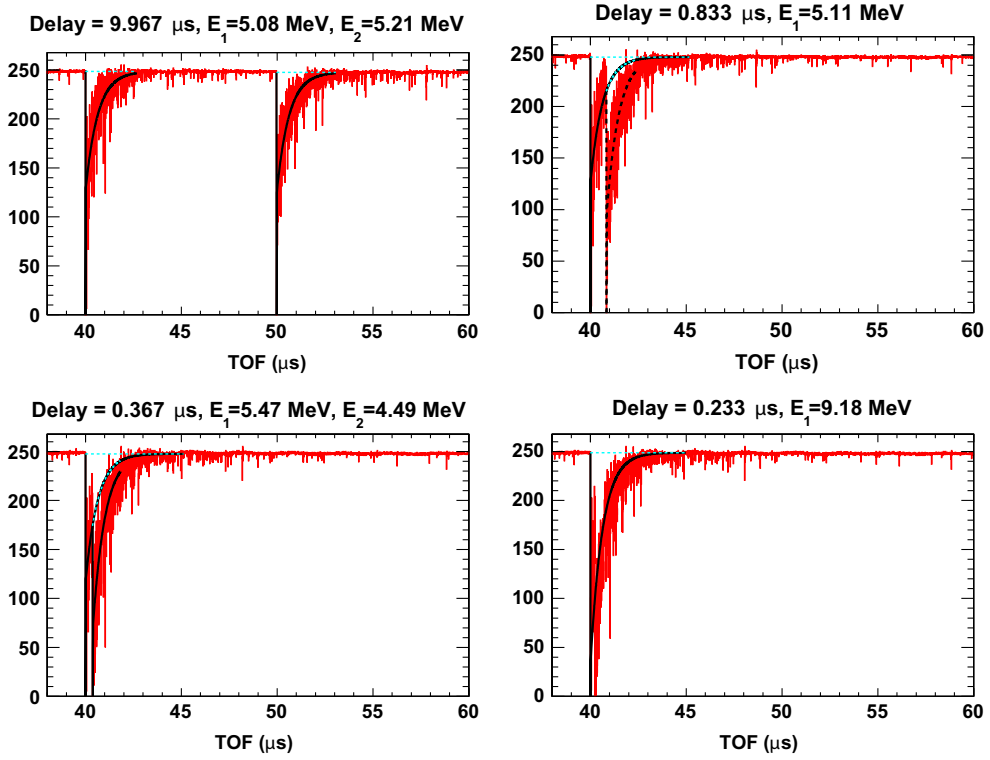

Fig. 7. Detection of the same signals with energies of 5.08 and 5.21 MeV but separated by different time delays. Signals identified by the pulse shape analysis routine are fitted by solid lines, otherwise the original pulse shape is indicated by a dotted line. The energies obtained by the routine are indicated on top of each panel.

intervals described before. Then, 5000 pairs of signals were generated for each detector with 300 different time steps uniformly distributed between 0 and 10 μs. From the analysis of all buffers, the dead time was characterized

1. by a function, $P(E_1, E_2, \Delta t)$, which provides the probability that the pulse shape analysis routine does not detect a signal with energy E_2 which follows a signal with energy E_1 after a time delay Δt and
2. by probability distributions, $P_{\{E_1,E_2,\Delta t\}}(\xi)$, where ξ defines the change in the detected energy of the first signal, E_1, when the second signal with energy E_2 and separated by Δt is not detected. The change was parametrized as $E_1' = E_1 + \xi E_1$, where E_1 is the detected energy of the signal when it is isolated and E_1' when it is followed by the (non-detected) second signal.

In both cases the results were averaged over the 40 BaF_2 crystals. For the $P(E_1, E_2, \Delta t)$ function, the energy values, E_1 and E_2, were discretized in the 27×27 energy interval pairs, and the Δt values in the 300 time steps. For each energy interval pair, ten different $P_{\{E_1,E_2,\Delta t\}}(\xi)$ distributions were obtained, one for each Δt interval uniformly distributed between 0 and 2 μs. Examples of

the $P(E_1, E_2, \Delta t)$ projections are presented in Fig. 8 and Fig. 9. As expected, the higher the first signal, the lower is the detection probability of the second one, and vice versa. Examples of $P_{\{E_1,E_2,\Delta t\}}(\xi)$ distributions are given in Fig. 10. One finds that for very small values of Δt most events are interpreted as the sum of the the two γ-rays, but that the method starts to work rather well as soon as the time difference is longer than about 0.5 μs.

The method was validated using capture cascades from a TAC measurement on ^{197}Au(n,γ) [7,12]. Two different deposited energy spectra have been constructed, assuming a low (0.1 reactions/μs) and high (1.0 reactions/μs) reaction rates. The simulation process described in Section 3 was used to reproduce both experimental results.

Because both spectra contained the same capture cascades, they differed only by the dead time effects. As shown in Fig. 11, the experimental spectra are well reproduced, thus confirming that the dead time corrections are properly treated in the simulation. A simulation for a count rate of $2\,\mu s^{-1}$ has been included to illustrate the strong increase of the dead time corrections from 0.7% to 20% and 60% in the examples of Fig. 11.

One should notice that the manipulation offline of isolated signals allows a more detailed description of the dead time effects than the one presented here, where only the $P(E_1, E_2, \Delta t)$ and $P_{\{E_1,E_2,\Delta t\}}(\xi)$ functions have been obtained. In particular, it is possible to parametrize different functions for each detector, instead of averaging them, or take into account other effects such as the change in the recontructed energy when two signals are close and both are detected (bottom-left panel of Fig. 7).

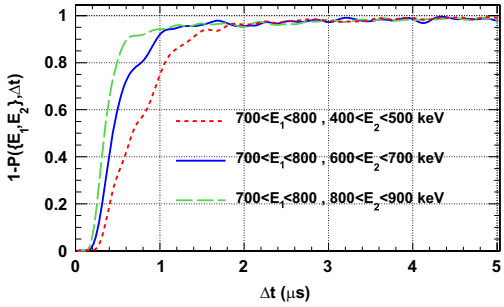

Fig. 8. Probability $1-P(E_1, E_2, \Delta t)$ for selected energy interval pairs.

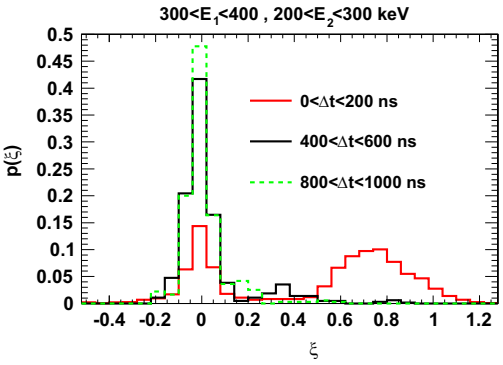

Fig. 10. Examples of $P_{\{E_1,E_2,\Delta t\}}(\xi)$ distributions, for two fixed energy interval pairs and different Δt intervals.

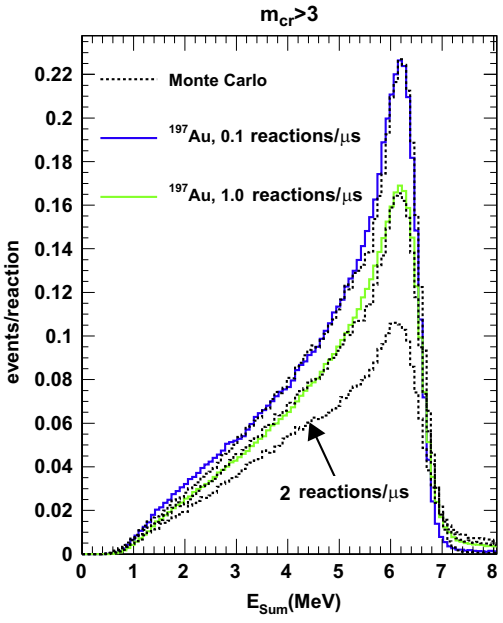

Fig. 11. Deposited energy spectra in the TAC for $m_{cr} > 3$ due to neutron capture cascades in ^{197}Au compared to Monte Carlo simulations for capture rates of 0.1, 1 and $2\,\mu s^{-1}$. The normalization of the Monte Carlo spectra to the experimental ones was performed with the corresponding $m_{cr} > 0$ histograms.

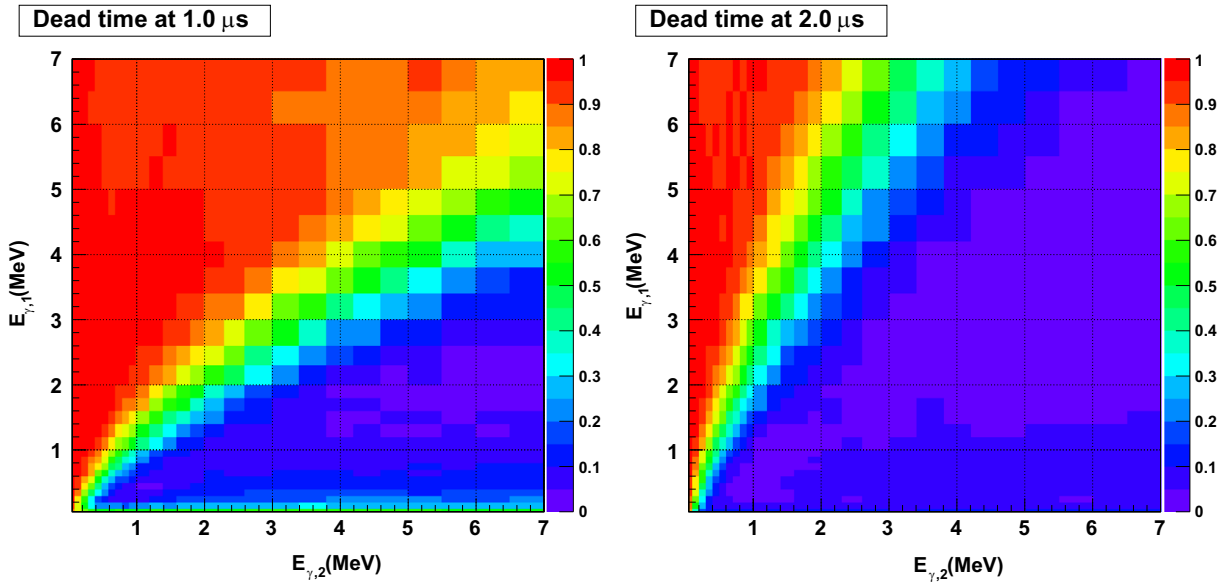

Fig. 9. Probabilities for not detecting a signal of energy E_2, which follows a signal of energy E_1 after 1 and 2 μs, respectively.

Finally, it should be noticed that we did not discuss the problem of a rapidly varying count rate. This case will be treated in a forthcoming paper [13].

5. Summary and conclusions

In this paper we have described techniques developed to characterize and correct three different dead time effects caused by pulse pile-up in an ^{243}Am(n,γ) measurement performed with the n_TOF Total Absorption Calorimeter.

The first correction allows one to transfer the effect of the ^{243}Am activity to independently measured background spectra, the second concerns the distortion of the detected ^{243}Am capture events by the sample activity, and the third correction deals with pile-up of capture events at very high count rates.

The three techniques are based on the same principle, which is the offline manipulation of the digitized detector signals and the parametrization of the response of the pulse shape analysis routine, showing the powerful capabilities of using digital electronics in counting experiments. In combination with detailed Monte Carlo simulations of the setup, accurate pile-up corrections have been obtained as it was verified by means of experimental information from (n,γ) measurements on ^{243}Am, ^{197}Au, and ^{nat}Ti. These techniques could be applied to other measurements for which the full digital information of the detectors is recorded and processed offline.

Acknowledgments

This work was supported partially by the Spanish national company for radioactive waste ENRESA, through the CIEMAT-ENRESA agreements on “Transmutación de residuos radiactivos de alta actividad”, the Spanish Plan Nacional de I+D+i de Física de Partículas (project FPA2008-04972-C03-01), the Spanish Ministerio de Ciencia e Innovación through the CONSOLIDER CSD 2007-00042 project and the European Union's Seventh Framework Programme under grant agreement no 262010.

References

[1] CERN n_TOF Facility: Performance Report. CERN INTC-2002-037, 2003.
[2] C. Guerrero, et al., Nucl. Inst. Met. A 608 (2009) 424.
[3] U. Abbondanno, et al., Nucl. Inst. Meth. A 538 (2005) 692.
[4] E. Berthoumieux, Preliminary Report on BaF2 Total Absorption Calorimeter Test Measurement, Rap. Tech., CEA-Saclay/DAPNIA/SPhN report, 2004.
[5] S. Marrone, et al., Nucl. Inst. Meth. A 568 (2006) 904.
[6] C. Guerrero, et al., Nucl. Inst. Meth. A 671 (2012) 108.
[7] C. Guerrero, et al., Phys. Rev. C 85 (2012) 044616.
[8] E. Mendoza, et al., Measurement of the ^{241}Am and the ^{243}Am Neutron Capture Cross Sections at the n_TOF Facility at CERN, Proceedings of the ND2013 Conference, to be published in Nucl. Data Sheets Jour. in 2014.
[9] E. Mendoza, et al., Phys. Rev. C 90 (2014) 034608.
[10] J.L. Taín, D. Cano-Ott, Nucl. Inst. Meth. A 571 (2007) 719.
[11] S. Agostinelli, et al., Nucl. Inst. Meth. A 506 (2003) 250.
[12] R. Macklin, et al., Nucl. Inst. Meth. 164 (1979) 213.
[13] C. Guerrero, D. Cano-Ott, E. Mendoza, Correction of dead-time and pile-up in detector arrays for constant and rapidly varying counting rates, to be submitted to Nucl. Inst. Meth. A.